Levitating atmospheres of Eddington-luminosity neutron stars

MNRAS **000**, 1–9 (2015) Preprint 5 April 2016 Compiled using MNRAS LATEX style file v3.0

Levitating atmospheres of Eddington-luminosity neutron stars

Maciek Wielgus,[1]★ Aleksander Sądowski,[2,3]† Włodek Kluźniak,[1]‡
Marek Abramowicz[1,4,5] and Ramesh Narayan[3]
[1]*Nicolaus Copernicus Astronomical Center, ul. Bartycka 18, 00-716, Warszawa, Poland*
[2] *MIT Kavli Institute for Astrophysics and Space Research, 77 Massachusetts Ave, Cambridge, MA 02139, USA*
[3]*Harvard-Smithsonian Center for Astrophysics, 60 Garden Street, Cambridge, MA 02138, USA*
[4] *Physics Department, Gothenburg University, 412-96 Goteborg, Sweden*
[5] *Institute of Physics, Faculty of Philosophy and Science, Silesian University in Opava, Bezrucovo nam. 13, 746-01 Opava, Czech Republic*

Accepted XXX. Received YYY; in original form ZZZ

ABSTRACT

We construct models of static, spherically symmetric shells supported by the radiation flux of a luminous neutron star in the Schwarzschild metric. The atmospheres are disconnected from the star and levitate above its surface. Gas pressure and density inversion appear in the inner region of these atmospheres, which is a purely relativistic phenomenon. We account for the scattering opacity dependence on temperature green by using the Klein-Nishina formula. The relativistic M_1 closure scheme for the radiation tensor provides a GR-consistent treatment of the photon flux and radiation tensor anisotropy. In this way we are able to address atmospheres of both large and moderate/low optical depths with the same set of equations. We discuss properties of the levitating atmospheres and find that they may indeed be optically thick, with the distance between star surface and the photosphere expanding as luminosity increases. These results may be relevant for the photosphereric radius expansion X-ray bursts.

Key words: gravitation – stars: neutron – stars: atmospheres – X-rays: bursts.

1 INTRODUCTION

This paper discusses the structure of spherically symmetric, static, shell-like atmospheres of extremely luminous, compact, non-rotating stars. The results are expected to be relevant to the astrophysics of accreting neutron stars.

Under certain conditions neutron stars may become so luminous that the forces associated with radiation may exceed the pull of gravity. Several systems with super-Eddington luminosity have been reported (McClintock & Remillard 2006), the "LMC transient" A0535-668 (Bradt & McClintock 1983) being a particularly clear example. Super-Eddington luminosities may be achieved in some X-ray bursts (Strohmayer & Bildsten 2006), as well as during accretion of matter in a semidetached binary, especially in a ULX (Bachetti et al. 2014), or a detached binary with a Be star as the companion. At least in the case of X-ray bursts the radiation field is nearly spherically symmetric. In most cases, extended periods of time may occur in which the radiation field and the gas can be taken to be in a quasi-steady state, i.e., not varying on the dynamical time-scale. For these reasons we study the problem of extremely luminous neutron stars under the simplifying assumptions of steady-state conditions and spherical symmetry in the Schwarzschild metric.

★ E-mail: maciek.wielgus@gmail.com (MW)
† E-mail: asadowsk@mit.edu (AS)
‡ E-mail: wlodek@camk.edu.pl (WK)

Contemporary theoretical studies of neutron star atmospheres in X-ray bursts involve sophisticated, spectrally resolved, treatment of the radiation (Suleimanov et al. 2011, 2012). However, effects of general relativity (GR) are often neglected for simplicity. In fact, these may be quite important. The atmospheric structure of luminous stars in GR has been studied by Paczynski & Anderson (1986), who found that the atmosphere becomes very extended in the Klein-Nishina regime of scattering opacity. However, in the Thomson regime, as well as in the Newtonian solutions for either of the scattering regimes, the atmosphere is geometrically thin. Paczyński and Anderson's results show that in the case of very luminous neutron stars it would be inappropriate to expect, and simply speak of, relativistic "corrections" to Newtonian solutions. In fact, qualitatively new results may appear when GR effects are included.

In this paper we report the presence of a new type of atmospheric solution for neutron stars radiating at nearly Eddington luminosities, which is qualitatively different from the ones obtained in Newtonian physics. We find that fluid atmospheres of luminous stars in general relativity may have the form of a shell suspended above the stellar surface, with the maximum density of the atmosphere attained on a surface separated from the star by a "gap" in which the atmospheric density and pressure drop precipitously as the stellar surface is approached. Such shells may have already been observed in some X-ray bursts (in't Zand et al. 2011). A certain group of bursts indicate radiation-driven ejection of the neutron

star gaseous envelope, e.g., Tawara et al. (1984); White & Angelini (2001); Wolff et al. (2005). Our model is expected to be of particular interest for modelling these so called photospheric radius expansion (PRE) bursts (Lewin et al. 1993). Unlike most models of atmospheres of highly luminous sources, e.g., Kato & Hachisu (1994), the discussed solutions do not involve dynamical outflows. Our results also differ from the static extended atmospheres of Paczynski & Anderson (1986), which share with their more familiar Newtonian counterparts the property that the atmospheric density increases monotonically as the stellar surface is approached. The key property of our solutions is that neither the density nor the pressure is monotonic as a function of the radius. Analytical models of optically thin Thomson-scattering shells hovering above the stellar surface of luminous neutron stars were presented by Wielgus et al. (2015). In this paper we consistently treat atmospheres of both large and moderate optical depths.

The unusual shell-like structure of our atmospheric solutions can be readily understood as a consequence of the spatial characteristics of the radiation field and of gravity. In general relativity, unlike in Newtonian theory, the pull of gravity and the radiation flux have a different dependence on the radial distance from the star. One consequence of this is that the Eddington luminosity is not a distance independent concept—in fact, typically the flux of radiation has a stronger dependence on the radius than the effective gravity. Hence, for a sufficiently luminous star, the radiation force may balance gravity only at a particular radial distance (Phinney 1987). Effectively, the Eddington flux is attained only on a certain surface (Bini et al. 2009; Oh et al. 2010), which is spherical for a spherically symmetric star. We refer to this surface as the Eddington Capture Sphere, or ECS (Stahl et al. 2012; Wielgus et al. 2012). Inside this surface, radiation force on an ionized atom exceeds the pull of gravity, outside it gravity prevails. Thus, the ECS is a locus of stable equilibrium positions for test particles (Abramowicz et al. 1990; Stahl et al. 2012).

Clearly, an atmosphere may exist, which is centred on the ECS and thinning out in both directions, towards and away from the luminous star, with the gas pressure gradient balancing the difference between the pull of gravity and the radiation pressure. In the optically thin limit the radiation force is simply given by the flux of radiation coming from the central star times the opacity and analytic solutions may be found (Wielgus et al. 2015). Here, we turn our attention to shells of more general optical depth, which require a numerical treatment of the gas-radiation interaction. In our numerical scheme we follow Levermore (1984) and assume that the radiation tensor is isotropic not in the fluid frame, but in the "rest frame" of the radiation. This leads to the M_1 closure. A generalization of the M_1 scheme to GR has been given in Sądowski et al. (2013).

For convenience, we parametrize the luminosity of the star by the ratio of the luminosity observed at infinity to the Eddington luminosity,

$$\lambda = L_\infty / L_{\rm Edd}, \tag{1}$$

with the standard expression for the latter,

$$L_{\rm Edd} = 4\pi G M m_p c/\sigma_{\rm T} = 4\pi G M c/\kappa_{\rm T}\,, \tag{2}$$

for proton mass m_p, Thomson cross-section $\sigma_{\rm T}$, and Thomson scattering opacity $\kappa_{\rm T}$. In the Schwarzschild metric, with $|g_{tt}(r)| = 1-2GMc^{-2}/r$, the stellar luminosity at radius r is

$$L(r) = L_\infty \left(1-\frac{2GM}{rc^2}\right)^{-1}, \tag{3}$$

and a static balance between gravity and radiation force with Thomson scattering can only be achieved at one radius $r = R_{\rm ECS}$, with

$$R_{\rm ECS} \equiv R_{\rm S}\left[1-(L_\infty/L_{\rm Edd})^2\right]^{-1}\,, \tag{4}$$

Thus, in terms of the constant introduced in Eq. (1),

$$R_{\rm ECS}/R_{\rm S} = 1/(1-\lambda^2)\,. \tag{5}$$

Numerous authors have shown that test particles initially orbiting the star (at various radii) will settle on the spherical surface at $r = R_{\rm ECS}$, provided that

$$(1-R_{\rm S}/R_*)^{1/2} \le \lambda < 1\,, \tag{6}$$

their angular momentum having been removed by radiation drag (Bini et al. 2009; Sok Oh et al. 2011; Stahl et al. 2012). In fact, any point on the ECS is a position of *stable* equilibrium in the radial direction (and neutral equilibrium in directions tangent to the ECS surface, Stahl et al. 2012).

Unless indicated otherwise, throughout this paper we use geometrical units, $G = c = 1$, with $2M$ denoting the Schwarzschild radius $R_{\rm S} = 2GM/c^2$. In the numerical calculations we fix the mass and radius of the central spherical star to $M = 1.5M_\odot$, $R_* = 2.5R_{\rm S}$ (corresponding to $R_* = 11$ km), and consider atmospheres consisting of pure ionized hydrogen. All results are given for the Schwarzschild spacetime and the signature is assumed to be $(-+++)$.

2 TREATMENT OF RADIATION

When treating the radiation as a fluid propagating through a possibly optically thick atmosphere, we need to employ a general formulation of the coupled energy-momentum conservation equations for the radiation ($R^\mu_{\ \nu}$) and gas ($T^\mu_{\ \nu}$) stress-energy tensors. In relativistic four-notation, the equations take the form

$$(R^\mu_{\ \nu})_{;\mu} = -G_\nu\,, \tag{7}$$

$$(T^\mu_{\ \nu})_{;\mu} = G_\nu\,, \tag{8}$$

where G_ν denotes the radiation four-force density (Mihalas & Mihalas 1984), a coupling term between gas and radiation. In the orthonormal fluid rest frame (hereafter denoted with a hat), under the spherical symmetry assumption, the only non-zero components of $G^{\hat\mu}$ are $G^{\hat t}$ and $G^{\hat r}$, with

$$G^{\hat t} = \kappa_{\rm a}\rho(R^{\hat t\hat t} - 4\sigma T^4)\,, \tag{9}$$

$$G^{\hat r} = \chi\rho R^{\hat t\hat r}\,. \tag{10}$$

Here $\chi = \kappa_{\rm a} + \kappa_{\rm s}$ denotes the total opacity coefficient, $\kappa_{\rm a}$ is the frequency integrated absorption opacity, $\kappa_{\rm s}$ is the scattering opacity, σ is the Stefan-Boltzmann constant, and T and ρ are the temperature and rest-mass density of the gas. We neglect the transfer of energy by Compton scattering.

When a static, and spherically symmetric system is to be considered, only the radial derivatives are of interest. Eqs. (7)-(8) then become ordinary differential equations in the variable r. The "angular" components $R^{(\phi)(\phi)} = R^{(\theta)(\theta)}$ can be eliminated if one remembers that the radiation tensor has a vanishing trace, $R^\mu_{\ \mu} = 0$. We indicate components in the orthonormal Schwarzschild tetrad by indices in parentheses. Under our assumptions this tetrad coincides with the orthonormal fluid rest frame, hence $R^{\hat\mu\hat\nu} \equiv R^{(\mu)(\nu)}$. This simplifies the calculations greatly, so that Eq. (7) yields the following

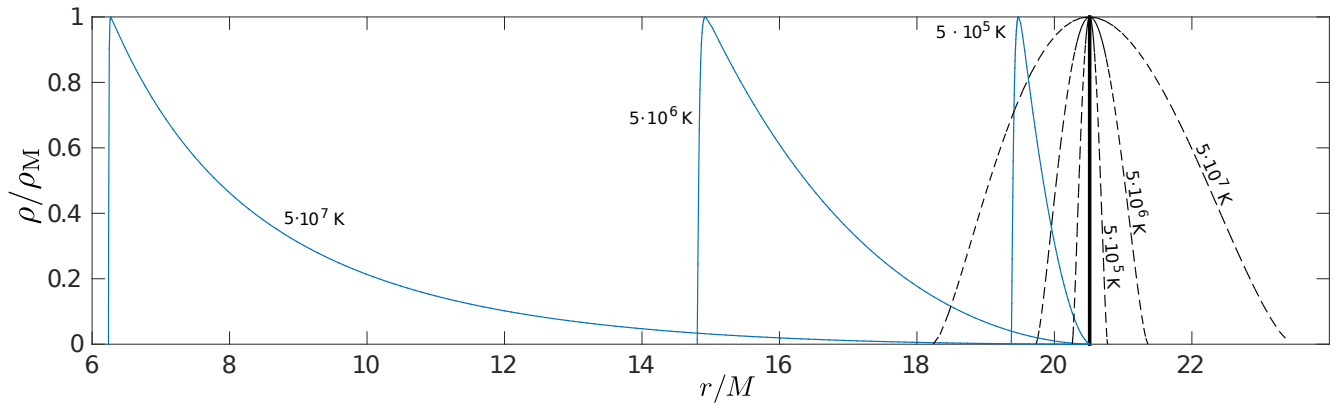

Figure 1. Comparison of density profiles for optically thin atmospheres found with Thomson scattering opacity (black, dashed lines) and Klein-Nishina scattering opacity (blue, continuous lines) for luminosity $\lambda = 0.95$. The maximum temperatures are: $T_M = 5\cdot10^5$K, $5\cdot10^6$ K, $5\cdot10^7$ K. Thick black continuous line denotes the test particle ECS location. For the Klein-Nishina atmospheres a significant reduction of the equilibrium radius $R_{\rm E}$ with temperature increase is observed.

system

$$\frac{1}{r^2}\frac{\mathrm{d}}{\mathrm{d}r}\left(r^2 R^r{}_t\right) = -G_t\,, \tag{11}$$

$$\frac{\mathrm{d}}{\mathrm{d}r}R^r{}_r = -\frac{(r-3M)R^t{}_t + (3r-5M)R^r{}_r}{r^2(1-2M/r)} - G_r\,. \tag{12}$$

In general, solving Eq. (12) requires knowledge of the radiative force term G_r, as well as the radiation energy density, which is given by $R^{(t)(t)} = -R^t{}_t$ in the Schwarzschild spacetime.

We will assume $G^{\hat{t}} = 0$ throughout this paper. Formally, from Eq. (9), this implies that either absorption is negligible or $R^{\hat{t}\hat{t}} - 4\sigma T^4 = 0$. The latter corresponds to the condition of local thermodynamic equilibrium (LTE).

Clearly, Eq. (11) is decoupled from the system when $G^{\hat{t}} = 0$. It gives the condition of zero flux divergence, with a simple solution

$$R^{(t)(r)}(r) = R^{tr}(r) = \frac{L_\infty}{4\pi r^2(1-2M/r)}\,. \tag{13}$$

With the radiative flux formula given by Eq. (13), the G_r component becomes

$$G_r = g_{rr}e^r_{(r)}G^{(r)} = g_{rr}e^r_{(r)}\chi\rho R^{(t)(r)} \tag{14}$$

where $e^r_{(r)} = |g_{rr}|^{-1/2}$ is a Schwarzschild tetrad coefficient. To solve Eq. (8) we assume an ideal gas and write the stress energy tensor as

$$T^\mu{}_\nu = (\rho + p + \epsilon)u^\mu u_\nu + \delta^\mu{}_\nu p\,, \tag{15}$$

where p and ϵ are the pressure and internal energy of the gas and u^μ is its four-velocity. Eq. (8) then becomes

$$\frac{\mathrm{d}p}{\mathrm{d}r} = \frac{-(\rho+p+\epsilon)M}{r^2(1-2M/r)} + G_r = \frac{-(\rho+p+\epsilon)M}{r^2(1-2M/r)} + \frac{\lambda(\chi/\kappa_T)\rho M}{r^2(1-2M/r)^{3/2}}\,. \tag{16}$$

Equation (16) describes the condition for hydrostatic equilibrium in the presence of gravitational attraction and a radiation force. Of course, both pressure and the internal energy of the gas contribute to the gravitational attraction in the relativistic framework.

In summary, in our system there are two unknown components, R^{tt} and R^{rr}, of the radiation stress-energy tensor, which are related by a single differential equation, Eq. (12), and several gas quantities (pressure, density,...) also related by one equation, Eq. (16). In order to solve for these quantities, it is necessary to make some additional assumptions, specifically to adopt an equation of state for the gas and a closure scheme for the radiation.

In the limit of an isotropic radiation tensor, where $\rho_{\rm rad} = -R^t{}_t = 3R^r{}_r = 3R^\theta{}_\theta = 3R^\phi{}_\phi = 3p_{\rm rad}$, summing Eqs. (12) and (16), we recover the familiar equation

$$\frac{\mathrm{d}p_{\rm tot}}{\mathrm{d}r} = \frac{-(\rho_{\rm tot}+p_{\rm tot})M}{r^2(1-2M/r)}\,, \tag{17}$$

where $p_{\rm tot}$ and $\rho_{\rm tot}$ denote total pressure and total energy density of the gas and radiation mixture, given by

$$p_{\rm tot} = p + p_{\rm rad}, \tag{18}$$

$$\rho_{\rm tot} = \rho + \epsilon + \rho_{\rm rad}\,. \tag{19}$$

Equation (17) is the correct relativistic hydrostatic balance equation of an *optically thick* gas - radiation mixture.

3 OPTICALLY THIN POLYTROPIC ATMOSPHERES

While this paper is mainly concerned with atmospheres of arbitrary optical depth, we will first briefly discuss the optically thin solutions. In this regime the radiation stress-energy tensor is known *a priori* (Abramowicz et al. 1990), rendering the radiation transfer description trivial. This suffices to solve for hydrostatic equilibrium of a polytrope, as the model reduces to the following simple system of equations (one ordinary differential equation supplemented by algebraic ones)

$$\frac{\mathrm{d}p}{\mathrm{d}r} = \frac{-(\rho+p+\epsilon)M}{r^2(1-2M/r)} + \frac{\lambda(\kappa_{\rm s}/\kappa_{\rm T})\rho M}{r^2(1-2M/r)^{3/2}}\,, \tag{20}$$

$$p = K\rho^\Gamma = (\Gamma-1)\epsilon = \rho\frac{k_B T}{\mu m_p}\,, \tag{21}$$

where K is the polytropic constant, the adiabatic index is taken to be $\Gamma = 5/3$, the mean molecular mass $\mu = 1/2$, and the Thomson scattering opacity $\kappa_{\rm T} = 0.4$ cm^2/g (these correspond to pure ionized hydrogen in the non-relativistic limit). We neglect absorption, but account for temperature dependence of the scattering coefficient, corresponding to the (averaged) Klein-Nishina scattering model, i.e., $\chi = \kappa_{\rm s} = \kappa_{\rm KN}(T)$. The following approximate scattering opacity formula (Buchler & Yueh 1976; Paczynski 1983; Lewin et al.

1993) is used[1],

$$\kappa_{\rm KN}(T) = \kappa_T \left[1 + \left(\frac{T}{4.5\cdot 10^8 K}\right)^{0.86}\right]^{-1} . \quad (22)$$

The system of equations (20)-(21) can be readily solved numerically. From Eq. (20) one finds the location of the pressure maximum,

$$R_{\rm E} = \frac{2M}{1-\lambda^2 a_1^2 a_2^2} , \quad (23)$$

with

$$a_1(T) = \kappa_{\rm s}(T)/\kappa_{\rm T} , \quad (24)$$

$$a_2(T) = \left[1 + \frac{k_B T}{\mu m_p c^2}\frac{\epsilon + p}{p}\right]^{-1} = \left[1 + \frac{k_B T_M}{\mu m_p c^2}\frac{\Gamma}{\Gamma - 1}\right]^{-1} , \quad (25)$$

where the temperature is taken at its maximum value, treated as an arbitrary constant parametrizing the family of solutions, $T = T_M \equiv T(R_{\rm E})$. Because of the relativistic correction $(p+\epsilon)$ to density in Eq. (20) and the opacity temperature dependence, the expression for $R_{\rm E}$ differs from that for the test particle $R_{\rm ECS}$ by the presence of the correction factors a_1, a_2. The first factor gives no correction ($a_1 = 1$) if the Klein-Nishina modification to the Thomson scattering is neglected ($\kappa_{\rm s} = \kappa_{\rm T}$). As long as the temperature is much lower than 1 GeV, or $T_M \ll 10^{13}$ K, the second correction, a_2, is insignificant, $|1 - a_2| \ll 1$.

For non-relativistic temperatures, i.e., when the temperature correction factors are equal to unity, $a_1 = 1 = a_2$, it is straightforward to find analytic solutions for optically thin atmospheres (Wielgus et al. 2015). In particular, for high luminosities the atmospheric shells are suspended above surface of the star, with the gas density falling off on both sides of the sphere on which it attains its maximum. The results obtained here are qualitatively similar in general, and virtually identical to the analytic solutions in the particular case $a_1 = 1$. Figure 1 compares atmospheres described in this section with the analytic results for polytropic optically thin Thomson scattering atmospheres, discussed in Wielgus et al. (2015), for the same set of maximum temperatures T_M and fixed luminosity $\lambda = 0.95$. Since the equations are homogeneous in density (and pressure, for a given temperature), we show density profiles normalized by $\rho_{\rm M} = \rho(R_E)$.

When the luminosity is close to Eddington the atmospheric shells are suspended much closer to the neutron star for Klein-Nishina solutions than would be the case for purely Thomson scattering, since the opacity decreases at high temperatures in the Klein-Nishina model. This is because at high luminosities the denominator of Eq. (23) is very small, and even a small correction to the luminosity parameter significantly changes the value of the denominator, and hence of the radius of equilibrium $R_{\rm E}$.

Furthermore, the radial atmospheric profile of the density becomes extremely asymmetric, the atmosphere falling off quite sharply towards the star, but being rather extended on the side away from the star (i.e., for $r > R_{\rm E}$) owing to the rapid growth of the running value of $a_1(T)$ as the scattering cross-section increases with decreasing temperature, the gradient of pressure in Eq. (20) being sensitive—at any radius r—to the difference $1 - \lambda a_1(T)$.

[1] We omit from the denominator of Eq. (22) an additional factor of $\left(1 + 2.7\cdot 10^{11}\rho/T^2\right)$, which is appropriate in the limit of degenerate matter.

4 OPTICALLY THICK LTE ATMOSPHERES

Observations show that the atmospheres of radius expansion X-ray bursts are optically thick, so any model aspiring to address these phenomena needs to allow for larger optical depths than the ones discussed in the previous section. This, in general, demands solving for the coupled interaction of radiation and gas exchanging energy and momentum through absorption and scattering.

4.1 Closure scheme for the radiation tensor

When absorption is the only process involved the interaction is local and solving the radiative transfer equation is straightforward. However scattering on electrons is often important (in the atmospheres of thermonuclear X-ray bursts it is even dominant), and the intrinsically non-local character of transport in that process renders Monte Carlo methods ineffective, at the same time necessitating the computationally expensive use of non-local scattering kernels in the radiative transfer equation.

To solve the equations of gas-radiation interaction and evolution one has to make certain assumptions. An effective approach is to replace the angle-dependent equation of radiative transfer with equations describing evolution of only the first few moments of the radiation field. Such an approach, however, requires a *closure scheme*, i.e., extra assumptions for calculating the missing components of the radiation stress-energy tensor.

The simplest approach is Eddington closure, which assumes an isotropic radiation field in the fluid frame, i.e.,

$$R^{\hat{r}\hat{r}} = R^{\hat{\phi}\hat{\phi}} = R^{\hat{\theta}\hat{\theta}} = \frac{1}{3}R^{\hat{t}\hat{t}} . \quad (26)$$

In this scheme the complete radiation tensor is determined by a single component, the radiation energy density R^{tt}. However, application of this closure scheme is limited to the optically thick regime. A more sophisticated approach is afforded by the M_1 closure, which assumes that the radiation stress-energy tensor is isotropic (and the radiative flux vanishes) in the orthonormal "rest frame" of the radiation (Levermore 1984). This statement is represented by the following system of equations (Sądowski et al. 2013),

$$R^{\mu\nu} = \frac{4}{3}\bar{E}u_R^\mu u_R^\nu + \frac{1}{3}\bar{E}g^{\mu\nu} , \quad (27)$$

where u_R^μ is the radiation rest frame four-velocity, while $\bar{E}$ is the radiation energy density in this frame. The system of Eqs. (27) can be solved uniquely at any given radius, provided that the radiation energy density R^{tt} and radiation fluxes $R^{t\mu}$ are known (the zeroth and first moments of the specific intensity). The procedure is to first calculate $\bar{E}$ and u_R^t, which involves solving two coupled quadratic equations. The solution is chosen uniquely under the assumption of $\bar{E} > 0$. The remaining components of u_R^ν are then evaluated from the corresponding components of Eq. (27) for $\mu = t$. Finally, the second moments of the specific intensity can be calculated.

In our case it is enough to find R^{rr} using the closure scheme,

$$R^{rr} = M_1\left(R^{tt}, R^{tr}\right) , \quad (28)$$

since under the assumption of spherical symmetry we can then evaluate $R^{\phi\phi}$ and $R^{\theta\theta}$ from the zero trace condition on $R^{\mu\nu}$.

4.2 Assumptions of the optically thick model

In this model we keep the time component of the radiative four-force G_t equal to zero, which is consistent with the LTE assump-

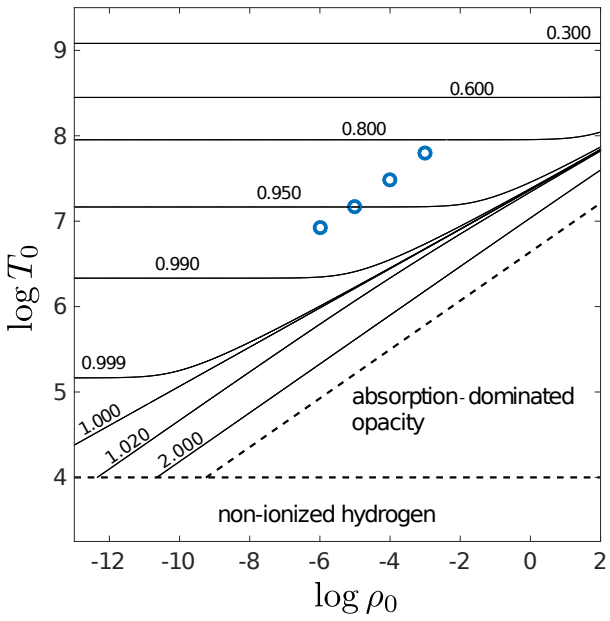

Figure 2. Contour plot of the a_3 correction factor, i.e., total opacity to Thomson scattering opacity ratio, Eq. (40), as a function of T_0 and ρ_0. Blue circles correspond to the four optically thick atmosphere solutions with $\lambda = 0.99$, shown in Fig. 4.

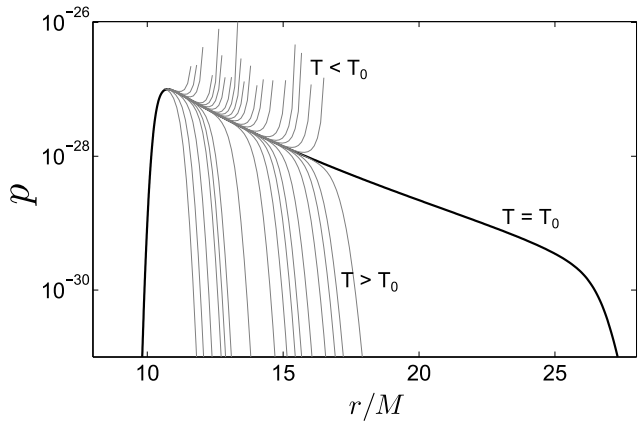

Figure 3. Example of a levitating atmosphere solution: radial distribution of pressure. Only one initial temperature, for a given choice of the other parameters, gives a solution which can be extended to infinity (thick black curve). Other choices of T_0 give solutions with an incorrect temperature at the photosphere (thin curves), and the pressure going either to infinity, or to zero at a finite radius R, with $R_0 < R < \infty$. Pressure in geometrical units.

tion,

$$\hat{E} \equiv R^{(t)(t)} = -R^t{}_t = 4\sigma T^4 \,, \tag{29}$$

corresponding to an atmosphere which has had enough time to relax to a steady state solution. In the opacity model we account for both absorption and scattering, $\chi = \kappa_a + \kappa_s$, where κ_a denotes the free-free (bremsstrahlung) opacity given in cgs units by Kramer's formula,

$$\kappa_a = 6.4\times 10^{22} T^{-7/2}\rho \,. \tag{30}$$

We also assume a mean molecular weight of $\mu = 1/2$ (pure ionized hydrogen).

Since temperatures of the order of $10^7 K$ are expected, in the scattering opacity we use the (direction and frequency averaged) Klein-Nishina opacity, $\kappa_s = \kappa_{KN}(T)$, as given by Eq. (22). Thus, κ_s is a decreasing function of the local gas temperature and equals the Thomson scattering opacity κ_T in the low temperature limit.

The system of equations describing our model is then as follows

$$\frac{dp}{dr} = \frac{-(\rho + p + \epsilon)M}{r^2(1-2M/r)} + G_r \,, \tag{31}$$

$$\frac{d}{dr}R^r{}_r = -\frac{(1-3M/r)R^t{}_t + (3-5M/r)R^r{}_r}{r(1-2M/r)} - G_r \,, \tag{32}$$

$$R^{tr}(r) = \frac{L_\infty}{4\pi r^2(1-2M/r)} \,, \tag{33}$$

$$G_r = \chi\rho(1-2M/r)^{1/2}R^t{}_r \,, \tag{34}$$

$$p = \frac{k_B}{\mu m_p}\rho T = \frac{2}{3}\epsilon \,, \tag{35}$$

$$T = \left(-\frac{R^t{}_t}{4\sigma}\right)^{1/4} \,, \tag{36}$$

$$R^{rr} = M_1(R^{tt}, R^{tr}) \,, \tag{37}$$

$$\chi = \kappa_a(T,\rho) + \kappa_{KN}(T) \,. \tag{38}$$

The system of Eqs. (31)-(38) can be solved uniquely for the six unknowns, $\rho, p, \epsilon, T, R^t{}_t$, and $R^r{}_r$, as functions of radius. Equating the right hand side of Eq. (31) to zero we find that the radius at which the gas pressure attains a maximum is

$$R_0 = \frac{2M}{1-\lambda^2 a_3^2 a_2^2}, \tag{39}$$

where a_2 is a temperature correction similar to the one present for the polytropic optically thin model, given by Eq. (25) with T_M replaced by $T_0 \equiv T(R_0)$, and a_3 is a new correction factor, reflecting the more general radiation transfer model assumed,

$$a_3 = \chi(R_0)/\kappa_T \,. \tag{40}$$

As already remarked, to high precision $a_2 = 1$ at temperatures prevalent in astrophysical neutron stars. However, the value of the a_3 parameter has a crucial influence on the position of an optically thick levitating atmosphere. For high temperatures, the opacity assumes low values because of the Klein-Nishina cross-section reduction and a much larger flux is required to balance gravity. On the other hand, dense gas at relatively low temperatures is characterized by large opacities, because of large absorption. In Fig. 2 a contour plot of the a_3 correction factor as a function of the model parameters is shown.

For the optically thick models considered here, in general, the radial positions of the density and pressure peaks do not coincide. The problem is no longer homogeneous in p and does not admit barytropic solutions. Thus, we need to specify two thermodynamic quantities as boundary values specifying the problem in order to perform the numerical integration. We parametrize the solutions with $[T_0, \rho_0, \lambda]$, i.e., with the temperature at the pressure maximum, T_0, density at the pressure maximum, $\rho_0 \equiv \rho(R_0)$, and the luminosity parameter λ of Eq. (1). The initial integration conditions $[p(R_0), R^r{}_r(R_0)]$ are calculated from the specified parameters using the ideal gas equation of state (pressure) and the LTE condition with M_1 closure (from T_0 we find R^{tt} using the LTE condition and we evaluate $R^r{}_r$ via the M_1 closure). This procedure fixes the values of all physical quantities at R_0, including the temperature and opacity corrections a_2, a_3, from which R_0 itself can be determined, whereupon the system of Eqs. (31)-(38) can be integrated in both directions, starting at $r = R_0$.

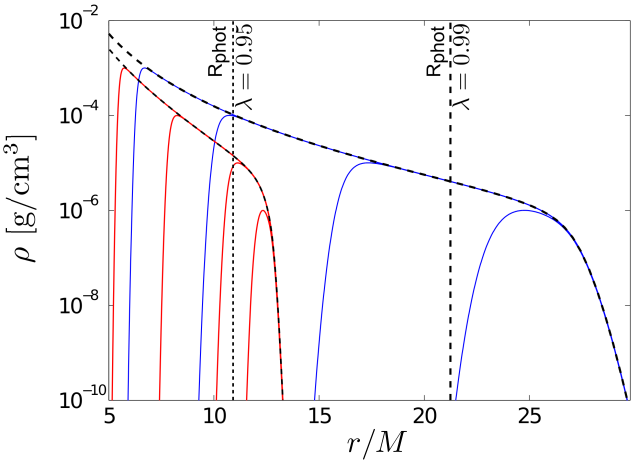

Figure 4. Comparison of the density profiles for luminosity $\lambda = 0.95$ (family of less extended red curves) and $\lambda = 0.99$ (family of more extended blue curves). The common envelopes of these two families of curves are indicated with dashed black lines. Corresponding locations of photospheres for each family are indicated with the vertical dashed lines. Test particle ECS for such luminosities are located at $20.5M$ and $100.5M$, respectively. This significant reduction of the equilibrium radius is due to the Klein-Nishina effect.

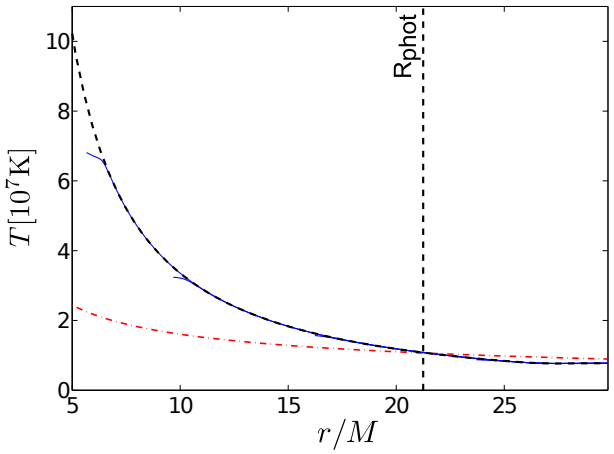

Figure 5. Temperature as a function of radius for LTE atmospheric shells with $\lambda = 0.99$. The common envelope indicated with dashed black line, red dash-dotted line corresponds to the effective temperature. Photosphere location indicated with a vertical dashed line.

4.3 Outer boundary condition

Although the system of Eqs. (31)-(38) can be solved for any choice of initial parameters (ρ_0, T_0), as described in the previous subsection, most of the solutions thus obtained would be unphysical, as the luminosity at infinity would bear no relation to the temperature of the photosphere. We need to impose an additional condition, that at scattering optical depth unity, $\tau_{\rm sc} = 1$, the LTE temperature is equal to the effective temperature. Here,

$$\tau_{\rm sc}(r) = \int_r^\infty \rho(r')\kappa_{\rm KN}(r')(1-2M/r')^{-1/2}\,{\rm d}r' \,. \qquad (41)$$

In practice, it is enough to demand that the pressure is well behaved, it neither goes to infinity nor vanishes at finite radii. Thus, for any given initial value of density ρ_0, we can reject all trial values of initial temperature which yield solutions that cannot be extended to infinity. This determines the value of T_0 uniquely for any given ρ_0 (and fixed values of the basic parameters such as M and λ), as illustrated in Fig. 3, where the thick curve corresponds to the minimum value of T_0 among those that yield a finite solution.

To effectively find the correct solution we use a numerical relaxation routine assuming $R^{rr}/R^{tr} = 1$ at the outer boundary, which corresponds to the radiation tensor of a point source in vacuum. While this condition is an approximation (it is only rigorously fulfilled at infinity), we find that the details of the outer boundary condition have negligible influence on the solution in the region of significant gas density. See the Appendix for some additional comments on the outer boundary condition.

For any (fixed) value of the luminosity, $\lambda < 1$, we obtain a family of physical solutions, differing by the density parameter ρ_0, related to the total mass of the shell.

4.4 Properties of the optically thick solutions

We find that for a given luminosity λ, levitating atmospheres of optical depth $\tau_{\rm sc} > 1$ only exist in a limited range of the ρ_0 parameter (density at the pressure maximum). Values of the density ρ_0 that are too low yield optically thin solutions, values of ρ_0 that are too large yield solutions in which the density decreases monotonically with the radius (the atmosphere is supported by the surface of the star).

Examples of levitating atmosphere density profiles, found for $\lambda = 0.95$ and $\lambda = 0.99$, are shown in Fig. 4. In the direction towards the star, the atmosphere thins out rather rapidly, so that there is a clear and large gap between the stellar surface and the levitating atmosphere. Away from the star, the atmosphere may be quite extended, the thinning out being slower than exponential, until it becomes optically thin to scattering. In the optically thin outer region the density of the atmosphere decreases rapidly. For a given star (fixed M, L_∞), the base of the levitating atmosphere can be located over a wide range of radii outside the star, with its position being determined by the total mass of the atmosphere, related to ρ_0. In the region of monotonic decrease of $\rho(r)$ all solutions coincide with a common envelope. The envelope, shown in Figs. 4-6 with thick black dashed lines, corresponds to the limit of a monotonic (non-levitating) solution, with no density inversion (formally $R_0 < R_*$).

Figure 5 illustrates the temperature as a function of radius for $\lambda = 0.99$ solutions. The red dash-dotted line corresponds to an effective temperature, $T_{\rm eff}(r) = [R^{tr}(r)/\sigma]^{1/4}$. The photosphere location, as found from the back integration of Eq. (41), is consistent with the surface at which the gas temperature is equal to the local effective temperature $T_{\rm eff}(r)$.

We find that the solutions are strongly dominated by the scattering opacity, as $\kappa_s/\kappa_a > 10^5$ for all radii. Radiation pressure strongly dominates over the gas pressure, with $p/p_{\rm rad} < 10^{-3}$ throughout the domain. The solutions vary from optically thin to scattering optical depths of the order of 10^3. Optical depths of solutions for $\lambda = 0.99$, calculated according to Eq. (41), are shown in Fig. 6. An obvious property of the levitating atmospheres is that there exists also an optically thin region in the inner part of the shell. It is located below a transition surface $r = R_{\rm tran}$, where the optical depth integrated *from the inside* is equal to unity, $\tau_{\rm in}(R_{\rm tran}) = \tau_{\rm sc}(R_*) - \tau_{\rm sc}(R_{\rm tran}) = 1$. These locations are indicated in Fig. 6 with blue dots.

The set of universal density profile envelopes, parametrized with λ, is shown in Fig. 7. Since the properties of these envelopes do not depend on ρ_0, the location of the photosphere is common to all the

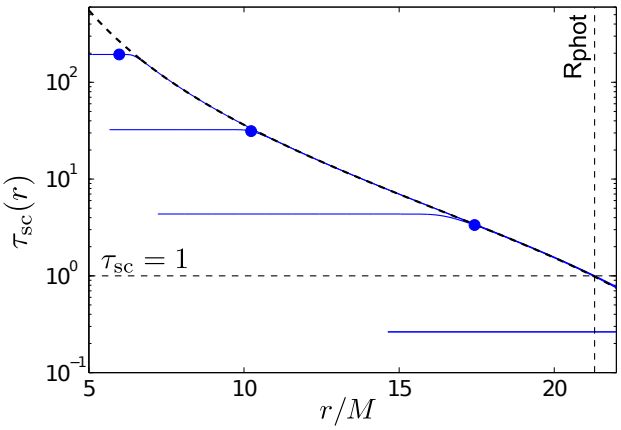

Figure 6. Integrated optical depth of the levitating atmospheres obtained for $\lambda = 0.99$. Dots indicate locations of the inner transition surface R_{tran}. The vertical dashed line is the common location of the photosphere.

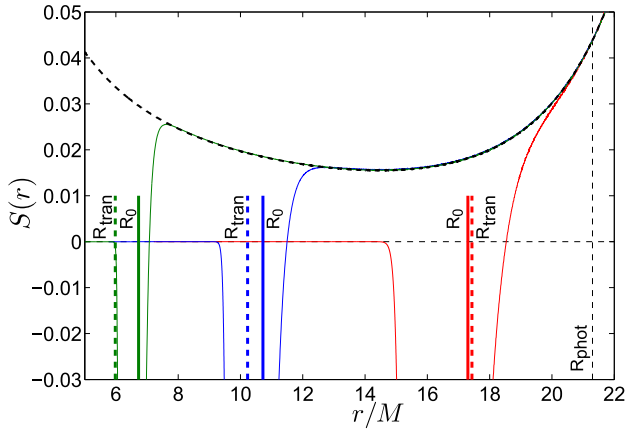

Figure 8. Schwarzschild stability criterion for the levitating atmospheres of $\lambda = 0.99$. The negative values indicate possible convective instability. Curves for the density parameter $\rho_0 = 10^{-3}, 10^{-4}, 10^{-5}$g/cm^3 (left to right).

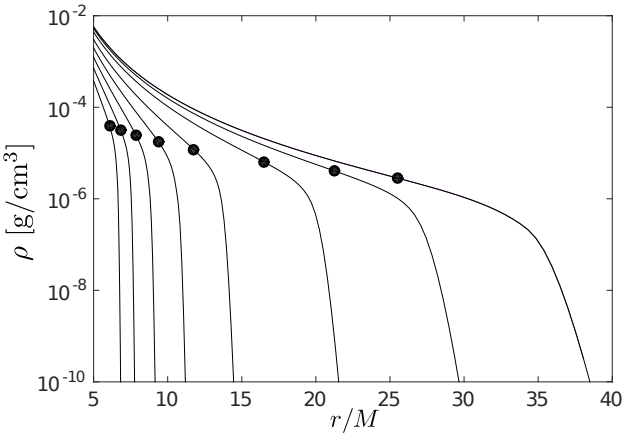

Figure 7. The envelopes of the atmospheric shells for various values of the luminosity. From left to right $\lambda = 0.88, 0.90, 0.92, 0.94, 0.96, 0.98, 0.99, 0.995$. Black dots indicate the position of the photosphere.

optically thick solutions at fixed M, L_∞ and tends to larger radii as luminosity increases, cf. Fig. 9.

4.5 Stability of LTE solutions

Convective stability of an optically thick relativistic atmosphere is determined by the Schwarzschild stability criterion (Thorne 1966),

$$S(r) = \frac{1}{\Gamma}\frac{\mathrm{d}\log p_{\rm tot}}{\mathrm{d}r} - \frac{1}{\rho_{\rm tot}+p_{\rm tot}}\frac{\mathrm{d}\rho_{\rm tot}}{\mathrm{d}r} > 0\,, \qquad (42)$$

where the total pressure and density, $p_{\rm tot}$ and $\rho_{\rm tot}$, are calculated according to Eqs. (18)-(19). The condition (42) can be readily obtained by linearly perturbing our simplified equation (17). We use $\Gamma = 4/3$, since our atmospheres are strongly radiation pressure dominated ($p/p_{\rm rad} < 10^{-3}$).

In Fig. 8 we show the radial distribution of $S(r)$ for levitating atmospheres calculated for $\lambda = 0.99$, $\rho_0 = 10^{-3}, 10^{-4}, 10^{-5}$g/cm^3. Positive values of $S(r)$ correspond to convective stability of the outer region of the atmospheres. The limiting envelope of levitating atmospheric solutions (dashed black line) has $S(r) > 0$ everywhere. Figure 8 indicates marginal stability, $S(r) = 0$, in the region between the stellar surface and the inner edge of the levitating atmosphere, suspended above the star. This is in agreement with the analytic limit of $S(r)$ for pure radiation and zero gas density.

The situation in the inner region of the atmospheres is somewhat more complicated. While Fig. 8 formally indicates convective instability, $S(r) < 0$, near the transition radius $r = R_{\rm tran}$ the large optical depth condition is not met and hence the criterion itself is not strictly valid. Moreover, near-Eddington radiation flux is expected to have a strong stabilizing influence, damping the motion of the optically thin fluid, Stahl et al. (2013), and thus hindering the development of instabilities. For instance, Abarca & Kluźniak (in prep.) find that the fundamental radial mode of atmospheric oscillations is overdamped.

There clearly exists a necessity for a more general convective stability criterion, that would remain valid regardless of the optical depth. This, however, is beyond the scope of this work and will be a subject of future investigations.

5 DISCUSSION: PHOTOSPHERIC RADIUS EXPANSION BURSTS

The main result of this paper is that the atmospheres of luminous neutron stars may form static shells, suspended above the neutron star surface by the force of radiation. These shells may be optically thick or thin, depending on the amount of matter forming the shell, presumably ejected from the neutron surface in a luminous burst of thermonuclear origin.

Even if enough matter is ejected to initially form an optically thick atmosphere, it may easily become optically thin as luminosity increases and the envelope expands (if an envelope of fixed mass M_e is expanding, its optical depth goes down approximately with the inverse square of radius). This further justifies the necessity of a model capable of addressing properly the regime of optically thick gas and possible transition to the optically thin regime. An interesting feature of our model is that if the photosphere is formed, its properties (location, temperature) only depend on the luminosity parameter λ and not on the mass of the envelope.

A certain group of X-ray bursts exhibit particularly strong peak luminosities, approaching the Eddington limit (Lewin et al. 1993; Strohmayer & Bildsten 2006). A strong radiative force may push the gaseous envelope of the neutron star away from the stellar surface. In some luminous bursts it is observed that the emitting

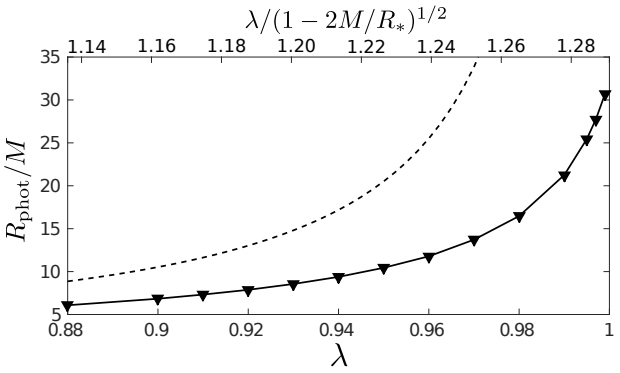

Figure 9. Photosperic radius, $R_{\rm phot}$ and the test particle Eddington capture sphere radius $R_{\rm ECS}$ (dashed lines).

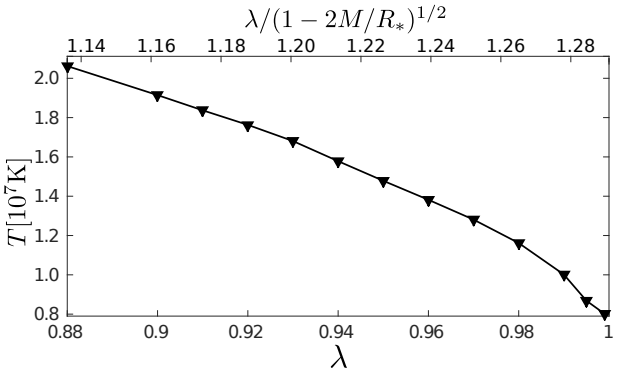

Figure 10. Photospheric temperature as a function of luminosity λ.

surface, inferred from the effective temperature and the luminosity, increases during the early stages of the bursts and then decays to its initial value during the so called touch-down phase. This group of bursts is referred to as PRE bursts. It was argued that the burst luminosity almost exactly reaches the Eddington luminosity during the expansion phase, (Kato & Hachisu 1994). The main argument to support this strong claim is that any excess energy from super-Eddington flux would be efficiently converted to kinetic energy, resulting in dynamical outflows. Sub-Eddington flux could not, on the other hand, explain the photospheric radius expansion, inferred from the observed spectra.

Observations of PRE bursts can reveal important knowledge about the dependence between neutron star mass and radius (Damen et al. 1990; Özel 2006; Özel et al. 2015) and it is reasonable to expect that better understanding of the relations between luminosity, photosphere location and temperature in PRE bursts should provide more detailed insight. For instance, in the basic models, the location of the photosphere is assumed (Damen et al. 1990) to coincide with what was later recognized to be the test-particle Eddington capture sphere (Stahl et al. 2012). We find that this is a significant overestimation, since the photospheric radius of the levitating atmospheres is typically situated much closer to the stellar surface than the test particle ECS, (Fig. 9). We also observe that it is not necessary for the flux to be of Eddington value for the photosphere to start expanding. Figure 9 indicates that the expansion begins at luminosity about $0.85L_{\rm Edd}$ and progresses with the increase of luminosity. For luminosity equal to $0.99L_{\rm Edd}$ the photospheric radius expands by a factor of about 4, while simultaneously cooling down by a factor of 2, Fig. 10. This seems to be in agreement with a typical expansion magnitude inferred from the observational data, see, e.g., in't Zand et al. (2013). In Figs. 9 and 10 the horizontal axes are labelled with λ as used throughout this paper, as well as and with luminosity normalized by the factor of $L_{\rm Edd}(1-2M/R_*)^{1/2}$, corresponding to the equilibrium luminosity at the stellar surface $r = R_*$. We note that the discussed luminosities are mildly super-Eddington if the latter is adopted as an "Eddington luminosity" unit.

In conclusion, we suggest that detailed modelling of near-Eddington photospheric expansion bursts should take into account the effects described in this work.

ACKNOWLEDGEMENTS

We thank Omer Blaes, Feryal Özel, and David Abarca for interesting comments on the subject of this paper. This research was partly supported by Polish NCN grants UMO-2011/01/B/ST9/05439 and UMO-2013/08/A/ST9/00795 as well as the Czech ASCRM100031242 CZ.1.07/2.3.00/20.0071 "Synergy" (Opava) project. MW also acknowledges the support of the Foundation for Polish Science within the START programme.

REFERENCES

Abramowicz M. A., Ellis G. F. R., Lanza A., 1990, ApJ, 361, 470
Bachetti M., et al., 2014, Nature, 514, 202
Bini D., Jantzen R. T., Stella L., 2009, Classical and Quantum Gravity, 26, 055009
Bradt H. V. D., McClintock J. E., 1983, ARA&A, 21, 13
Buchler J. R., Yueh W. R., 1976, ApJ, 210, 440
Damen E., Magnier E., Lewin W. H. G., Tan J., Penninx W., van Paradijs J., 1990, A&A, 237, 103
Kato M., Hachisu I., 1994, ApJ, 437, 802
Levermore C. D., 1984, J. Quant. Spectrosc. Radiative Transfer, 31, 149
Lewin W. H. G., van Paradijs J., Taam R. E., 1993, Space Sci. Rev., 62, 223
McClintock J. E., Remillard R. A., 2006, Black hole binaries. pp 157–213
Mihalas D., Mihalas B. W., 1984, Foundations of radiation hydrodynamics
Oh J. S., Kim H., Lee H. M., 2010, Phys. Rev. D, 81, 084005
Özel F., 2006, Nature, 441, 1115
Özel F., Psaltis D., Guver T., Baym G., Heinke C., Guillot S., 2015, preprint, (arXiv:1505.05155)
Paczynski B., 1983, ApJ, 267, 315
Paczynski B., Anderson N., 1986, ApJ, 302, 1
Phinney E. S., 1987, in Zensus J. A., Pearson T. J., eds, Superluminal Radio Sources. pp 301–305
Sądowski A., Narayan R., Tchekhovskoy A., Zhu Y., 2013, MNRAS, 429, 3533
Sok Oh J., Kim H., Mok Lee H., 2011, New Astronomy, 16, 183
Stahl A., Wielgus M., Abramowicz M., Kluźniak W., Yu W., 2012, A&A, 546, A54
Stahl A., Kluźniak W., Wielgus M., Abramowicz M., 2013, A&A, 555, A114
Strohmayer T., Bildsten L., 2006, New views of thermonuclear bursts. pp 113–156
Suleimanov V., Poutanen J., Werner K., 2011, A&A, 527, A139
Suleimanov V., Poutanen J., Werner K., 2012, A&A, 545, A120
Tawara Y., et al., 1984, ApJ, 276, L41
Thorne K. S., 1966, ApJ, 144, 201
White N. E., Angelini L., 2001, ApJ, 561, L101
Wielgus M., Stahl A., Abramowicz M., Kluźniak W., 2012, A&A, 545, A123
Wielgus M., Kluźniak W., Sadowski A., Narayan R., Abramowicz M., 2015, MNRAS, 454, 3766
Wolff M. T., Becker P. A., Ray P. S., Wood K. S., 2005, ApJ, 632, 1099
in't Zand J. J. M., Galloway D. K., Ballantyne D. R., 2011, A&A, 525, A111

in't Zand J. J. M., et al., 2013, A&A, 553, A83

APPENDIX A: COMMENTS ON THE M_1 CLOSURE

In the limit of $M/r \to 0$ an analytic expression for the M_1 closure can be given

$$\frac{R^{rr}}{R^{tr}} = \frac{2-a^2+a(4a^2-3)^{1/2}}{a+(4a^2-3)^{1/2}}\ , \tag{A1}$$

where $a = R^{tt}/R^{tr}$. The corresponding curve is shown in Fig. A1. With Eq. (32) being a differential equation for the R^{rr} component, in this work we are actually interested in the "inverse M_1" problem, i.e., in finding the R^{tt} component, given R^{rr} and R^{tr} at every step of the numerical integration of Eq. (32). It is worth noticing that while the M_1 closure scheme is a unique procedure, it is not an injective function of (R^{tt}, R^{tr}), meaning that a given R^{rr} may correspond to more than one pair R^{tt}/R^{tr}, see Fig. A1. Closer inspection of the formula (A1) reveals that the minimum of the M_1 curve corresponds to $\beta = u^r_R/u^t_R = c/\sqrt{3}$ and separates the right "subsonic photon gas" optically thick branch from the left "supersonic photon gas" optically thin branch. The numerical relaxation procedure that we utilize is necessary for the solution to pass through that "sonic point", and allow for a continuous transition from the optically thick regime of radiation trapped in the gas to the optically thin regime of freely streaming photons, forced by the outer boundary condition.

We note that in vacuum for an isotropic radiation stress tensor, i.e., for $G_r = 0$ and $R^t{}_t = -3R^r{}_r$, Eq. (12) takes the form

$$\frac{\mathrm{d}}{\mathrm{d}r}R^r{}_r = -\frac{4M}{r^2(1-2M/r)}\,R^r{}_r, \tag{A2}$$

with the solution $R^r{}_r = p_0/(1-2M/r)^2$, where p_0 is an integration constant of dimension pressure. The energy density of this isotropic radiation field scales correctly with the fourth power of the redshift factor $(1+z)$:

$$R^{(t)(t)} = 3R^{(r)(r)} = 3p_0\left(1-\frac{2M}{r}\right)^{-2}. \tag{A3}$$

We find that in the region between the stellar surface and the atmosphere our numerical solutions follow Eq. A3 quite closely.

This paper has been typeset from a TEX/LATEX file prepared by the author.

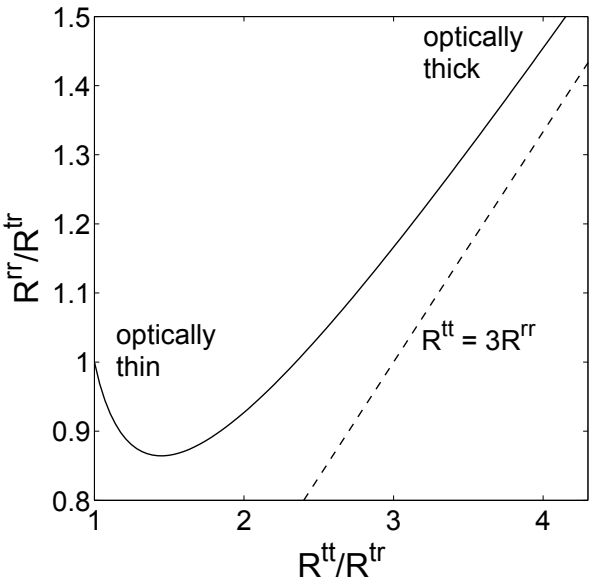

Figure A1. The ratio R^{rr}/R^{tr} versus R^{tt}/R^{tr} calculated with the M_1 scheme for $M/r \to 0$. Notice the non-injective character of the M_1 closure scheme in the optically thin regime.